XVII European Conference
ECSMGE 2019
Reykjavik
on Soil Mechanics
and Geotechnical Engineering

Pore pressure behavior of compacted clay under long-term cyclic loads in undrained conditions

Comportement des pressions interstitielles de l'argile compactée sous des charges cycliques à long terme dans des conditions non drainées

A. Głuchowski

Facullty of Civl and Environmental Engineering, Warsaw University of Life Sciences, Warsaw, Poland

W.Sas, E. Soból, K. Gabryś, A. Szymański

Facullty of Civl and Environmental Engineering, Warsaw University of Life Sciences, Warsaw, Poland

ABSTRACT: The phenomena of cohesive soils respond to cyclic loading is an important subject due to the fact of increasing demand to subgrade soils bearing capacity and deformation potential. The knowledge about soil respond to cyclic loading is important when design and service phase is considered by the designers. The conditions under which cohesive soil encounters most of the plastic deformations are undrained conditions and therefore main focus in this topic should be concentred on pore pressure behaviour. In this paper, cyclic triaxial test results are presented to characterize the development of undrained pore pressure. The tests were performed with an installed mid-plane pore pressure probe for more precise pore pressure measurements. The effects of deviator stress, confining pressure, initial porosity and plasticity on pore pressure are investigated. In this paper, an empirical model is proposed to predict the development of undrained pore pressure based on experimental data from the tests. This paper provides some innovative observations in order to better understanding undrained pore pressure behaviour of compacted clay under long-term cyclic loads.

RÉSUMÉ: Le phénomène des sols cohésifs réagissant à la charge cyclique est un sujet important en raison de la demande croissante pour le soubassement des sols et leur potentiel de déformation. Les connaissances sur les sols répondent aux charges cycliques sont importantes lorsque les concepteurs envisagent la phase de conception et d'exploitation. Les conditions dans lesquelles un sol cohésif rencontre la plupart des déformations plastiques sont des conditions non drainées; par conséquent, le sujet principal de ce sujet devrait être concentré sur le comportement de la pression interstitielle. Dans cet article, les résultats des essais triaxiaux cycliques sont présentés pour caractériser l'évolution de la pression interstitielle non drainée. Les tests ont été réalisés avec une sonde de pression interstitielle dans le fond de panier pour des mesures plus précises de la pression interstitielle. Les effets de la contrainte déviateur, de la pression de confinement, de la porosité initiale et de la plasticité sur la pression interstitielle sont étudiés. Dans cet article, un modèle empirique est proposé pour prédire le développement de la pression interstitielle non drainée sur la base des données expérimentales issues des tests. Ce document fournit des observations innovantes afin de mieux comprendre le comportement de la pression interstitielle non drainée de l'argile compactée sous des charges cycliques à long terme.

Keywords: cyclic loading, cohesive soil, pore pressure, excess pore pressure

1 INTRODUCTION

Excess pore water pressure is a key phenomena which impacts subgrade cohesive soils subjected to the traffic cyclic loading. The pore pressure development leads to stiffness degradation and to the development of ruts (Cary and Zapata 2014, Głuchowski et al. 2015).

The development of the pore pressure depends on factors which can be classified into three categories. First group constitutes a factors related to the stress state under which soil is acting. The second group consists of the repeating loading patterns and the last one is for factors describing the soil type (Cary and Zapata 2014, Fredlund 2006). The impact of stress state which can be further divided into impact of deviator stress or confining stress has been well studied so far (Brown et al. 1975, Ansal and Elken 1989, Mendoza and Hernandez 1994, Ichii and Mikami 2018). The impact of applied deviator stress has been found to be crucial for pore pressure development. A threshold deviator stress has been established which describes the different response of cohesive soil in the form of plastic strain and generated pore pressure under undrained conditions.

The impact of the repeating loading patterns on the pore pressure generation can be further divided into the impact of frequency and impact of the deviator stress amplitude. The frequency impact on the soil deformability and stiffness is greater with its increasing. The same behaviour was observed in the case of deviator stress amplitude (Sun 2018).

The last group of properties explains how cohesive soil physical properties impacts on the pore pressure generation. The plasticity index and fine particle content are most important in that case (Hsu and Vucetic 2006).

The cohesive soil which becomes a subgrade of newly founded construction is usually precompacted purposely or accidentally. This or another way, the natural soil composition is changed and the cohesive soil is acting as a preconsolidated one. Therefore, the tests of subgrade soils should be performed on compacted remoulded soil instead of the natural soil samples.

The cohesive soil sample subjected to cyclic loading will generate excess pore water pressure and therefore the effective stresses in the soil are going to decrease. Long term repeating loading may lead to such decrease of the effective stress p' that the failure will be observed.

In order to predict how excess pore water pressure develops during cyclic loading, the pore pressure generation models were proposed. An energy-based model proposed by Booker et al. (1976), was an empirical relation between dissipated shear energy and the residual excess pore water pressure ratio. The development of this model by Green et al. (2000) confirmed its usefulness in the case of stress-controlled cyclic loading tests.

The mathematical model proposed by Carry and Zapata (2014) was developed by analysis of the excess pore water pressure related to the time. The model is based on two curves which denote Global Cycle End Excess Pore Pressure and Global Peak Excess Pore Pressure. The pore pressure build-up is designed to reach asymptotic value. The results of the study lead to interesting conclusions concerning compaction techniques. The highly compacted cohesive soils tend to generate higher excess pore water pressure than less compacted ones.

The impact of pore pressure on cohesive soil response to cyclic loading is complex when additional physical factors are considered, as for example porosity-permeability variation. The Kozeny-Carman relationship was applied by Bayraktaroglu and Tasan (2018) in order to numerically simulate such behaviour in sandy soils. Results of the simulations have shown, that the porosity-permeability variation analysis is important and gives more accurate results.

In this article, the pore pressure generation of compacted cohesive soil is studied. The undrained cyclic triaxial tests were performed in a constant stress amplitude manner. The isotropic and consolidation was performed

before the tests. The excess pore water pressure is analysed as a function of axial strain and number of cycles.

2 MATERIALS AND METHODS

In this study sieve and aerometric (Bouyoucos method using a modification made by Casagrande) tests were carried on cohesive soil which was recognised as sandy silty clay (sasiCl), in accordance with EUROCODE 7 (PN-EN 14688:2006/Ap1). Soil used to conduct the tests was collected from a 1.2 m-deep earthwork construction site. The sand fraction f_{Sa} share was equal to 40%, silt fraction f_{Si} was equal to 42% and clay fraction f_{Cl} constitutes 18% of all soil mass. Test results are shown in Figure 1.
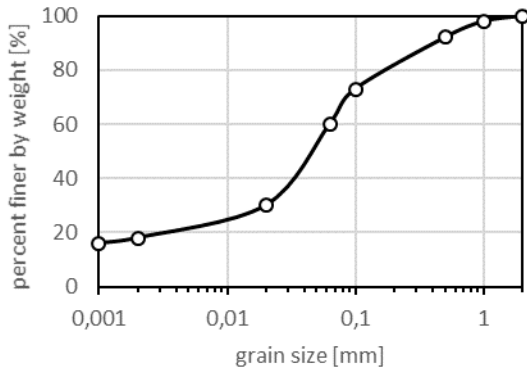
Figure 1. *Particle size distribution of tested soil.*

The Atterberg limits were established as well in this study. The liquid limit test was performed on the basis of five tests in Casagrande apparatus, with varying moisture content, the liquid limit was 41.5%. The plastic limit was equal to 23.1%. Therefore the plasticity index is equal to 18.4%.

The optimum moisture content was established with the Proctor test. The test was conducted by compaction of cohesive soil in the Proctor mould, with a volume equal to 2.2dm3 and by using standard energy of compaction, equal to 0.59J/cm2. Optimum moisture content

for sandy clay was 12.2% and maximum dry density at optimum moisture content reached 1.93g/cm3.

Additionally, the soil dynamic properties were conducted in order to establish the shear wave velocity VS. Table 1 presents the results of physical and mechanical tests on sandy silty clay.

Table 1. Physical and mechanical properties of sandy clay in this study.

Properties	Symbol	Value
Skeleton density	$\rho_s \ (g \cdot m^{-3})$	2.65
Dry density	$\rho_d \ (g \cdot m^{-3})$	1.93
Optimal moisture	$w_{opt} \ (\%)$	12.2
Liquid limit	$w_l \ (\%)$	23.1
Plasticity limit	$w_p \ (\%)$	41.5
Plasticity index	$Ip \ (-)$	18.4
Void ratio	$e_0 (-)$	0.375
S-wave velocity	$V_s \ (m \cdot s^{-1})$	244.5
Shear modulus	$G_0 \ (MPa)$	131.0

The tests were conducted in cyclic triaxial apparatus on seven samples with the diameter equal to 0.07 m and with the height equal to 0.14 m. The soil samples were compacted with the use of Proctor method in different moisture contents with OCR from 1.9 to 13.5. The specimens physical characteristic and test plan are present in Table 2.

Table 2. Physical properties and test plan for cohesicve soil samples in cyclic triaxial tests.

| Test No.	e_0 [-]	σ'_3 [kPa]	q_a [kPa]	q_m [kPa]	N [-]
1.1	0.41	45	4.1	39.5	$2 \cdot 10^4$
1.2	0.37	90	4.5	41.5	$2 \cdot 10^4$
1.3	0.41	135	3.95	39.2	$5 \cdot 10^4$
1.4	0.41	18	3.9	26.9	$5 \cdot 10^4$
1.5	0.59	46	2.6	25.6	$1 \cdot 10^4$
1.6	0.47	45	2.8	27.2	$5 \cdot 10^4$
1.7	0.41	90	2.75	27.3	$5 \cdot 10^4$

where: e_0 – initial void ratio, σ'_3 – minor principal effective stress during consolidation, q_a – deviator stress amplitude ($q_a = 0.5(q_{max} - q_{min})$) q_m deviator stress mendian ($q_m = 0.5(q_{max} + q_{min})$), N – number of cycles. Number of applied cycles N ranged from 10^3 to $5 \cdot 10^4$ and frequency of loading f was equal to 1 Hz.

3 TEST RESULTS

The results of the cyclic triaxial tests presented in this article were limited to the generation of excess pore water pressure and vertical strain development. Figs. 2 to 8 presents excess pore pressure Δu – vertical strain ε_1 characteristic.
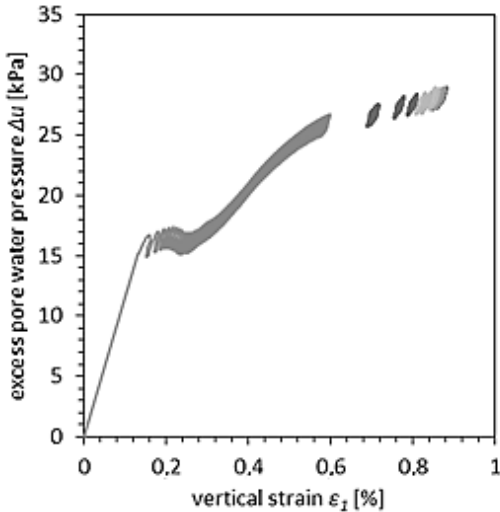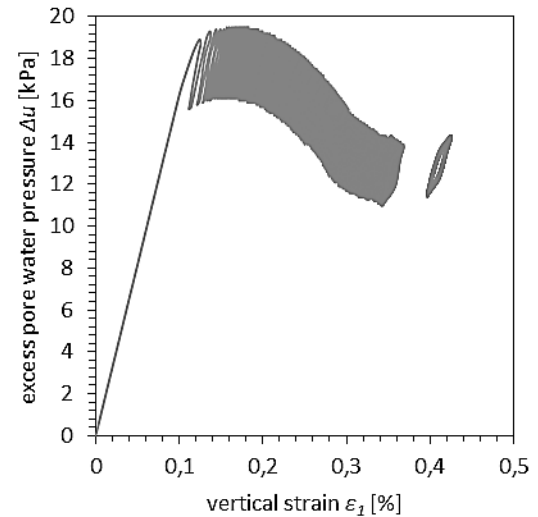

Figure 2. *Pore pressure characteristics for test 1.1, $q_a = 4.1$ kPa, $q_m = 39.5$ kPa, $\sigma'_3 = 45.0$ kPa.*
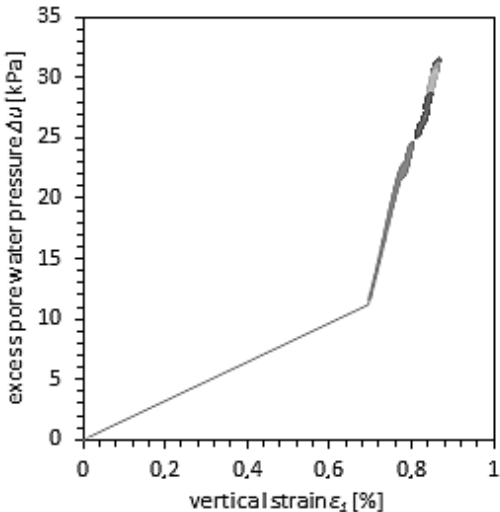
Figure 3. *Pore pressure characteristics for test 1.2, $q_a = 4.5$ kPa, $q_m = 41.5$ kPa, $\sigma'_3 = 90.0$ kPa.*
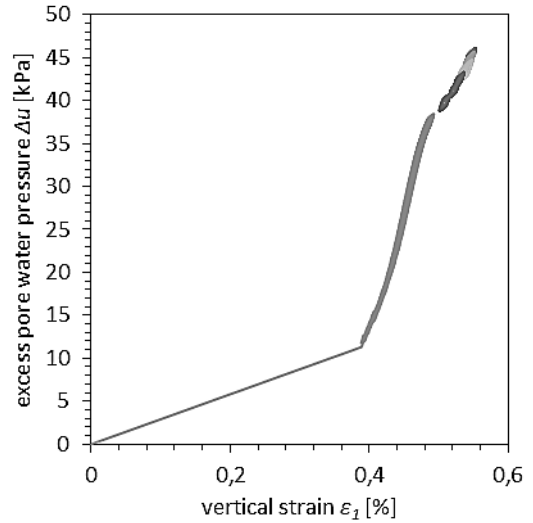
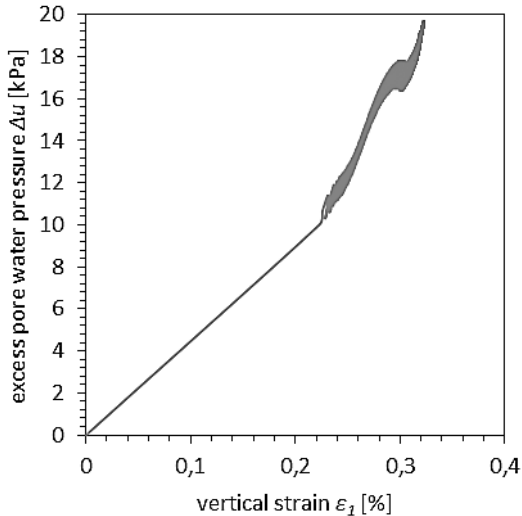**Figure 4.** *Pore pressure characteristics for test 1.3, $q_a = 3.9$ kPa, $q_m = 39.2$ kPa, $\sigma'_3 = 135.0$ kPa.*

Figure 5. *Pore pressure characteristics for test 1.4, $q_a = 3.9$ kPa, $q_m = 26.9$ kPa, $\sigma'_3 = 18.0$ kPa.*
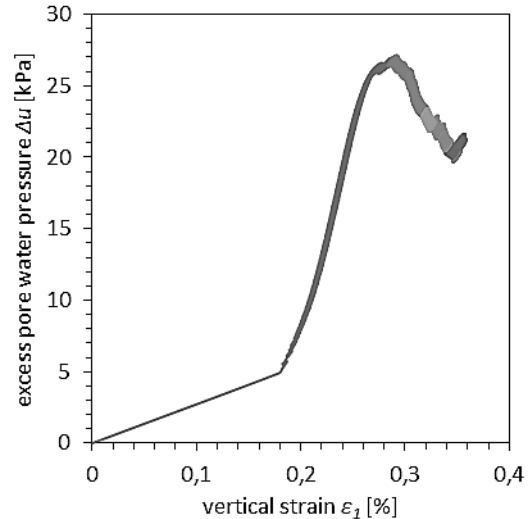
The excess pore pressure development has different characteristics The general rule which is common to all tests is rapid pore pressure development in the first cycle. This is reasonable since tested samples were consolidated in an isotropic manner. Analysis of the Figs. 2, 6 and 7 show a common pattern. In all three cases, the local maximal pore pressure exists. After in the Δu value decreases to a local

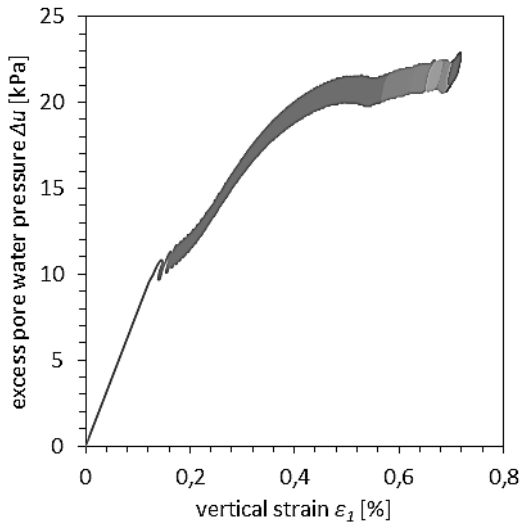minimum and after this occurrence, pore pressure rises again.

Figure 6. Pore pressure characteristics for test 1.5, $q_a = 2.6$ kPa, $q_m = 25.6$ kPa, $\sigma'_3 = 46.0$ kPa.

Figure 7. Pore pressure characteristics for test 1.6, $q_a = 2.8$ kPa, $q_m = 27.2$ kPa, $\sigma'_3 = 45.0$ kPa.

All three tests were performed in the same minor principal effective stress σ'_3 conditions equal to around 45.0 kPa. The local minimum Δu can be observed in different vertical strain.

conditions and the value of Δu also are different for each test.

Figure 8. Pore pressure characteristics for test 1.7, $q_a = 2.75$ kPa, $q_m = 27.3$ kPa, $\sigma'_3 = 90.0$ kPa.

In case of test 1.1, the local Δu maximum was observed in 17.5 kPa and $\varepsilon_1 = 0.2\%$, 17.5 kPa and 0.29% for the test 1.5 and 21.5 kPa, 0.48 for the test 1.6 respectively. After local Δu minimum, the pore pressure is rising. Pore pressure development had the greatest increment in case of test 1.1 where Δu raised to 28.9 kPa. This is because of high cyclic deviator stress. Tests 1.5 and 1.6 had closest stress state conditions. The only difference is the initial void ratio e_0 value. In test 1.5, the e_0 is equal to 0.59 and in test 1.6, the e_o equals 0.47. This difference resulted in higher excess pore pressure and axial strain development in case of test with smaller e_0 value.

The conclusion, from the above analysis, the higher compacted, the soil is the greater excess pore pressure will be developed. This statement is only valid in undrained conditions. Nevertheless, cyclic loading with the frequency equal to 1 Hz will certainly cause undrained conditions in cohesive soils.

Fig. 5 presents conditions with small minor effective principal stress σ'3 equal to 18.0 kPa.

The high cyclic deviator stress value caused the failure of the sample after a few repetitions. Nevertheless, further cyclic loads were conducted in order to find post-failure behaviour.

After $5 \cdot 10^4$ cycles, the excess pore water pressure stabilized itself and no further plastic vertical strains were observed. Figs. 3, 4 and 8 present the cyclic triaxial tests in higher σ'_3 value. The respond of cohesive soil to cyclic loading, in this case, was similar in all three cases. The excess pore water pressure has reached higher values when compared to the Δu in lower σ'_3 conditions. The first cycle in those tests had the most degrading effect in terms of pore pressure generation as well as in terms of caused vertical strain. The effect of cyclic loading on the pore pressure and vertical strain development can be considered for the last cycle. On Fig. 9 the $\Delta u - \varepsilon_1$ relationship for $1 \cdot 10^3$ cycle of loading was presented.
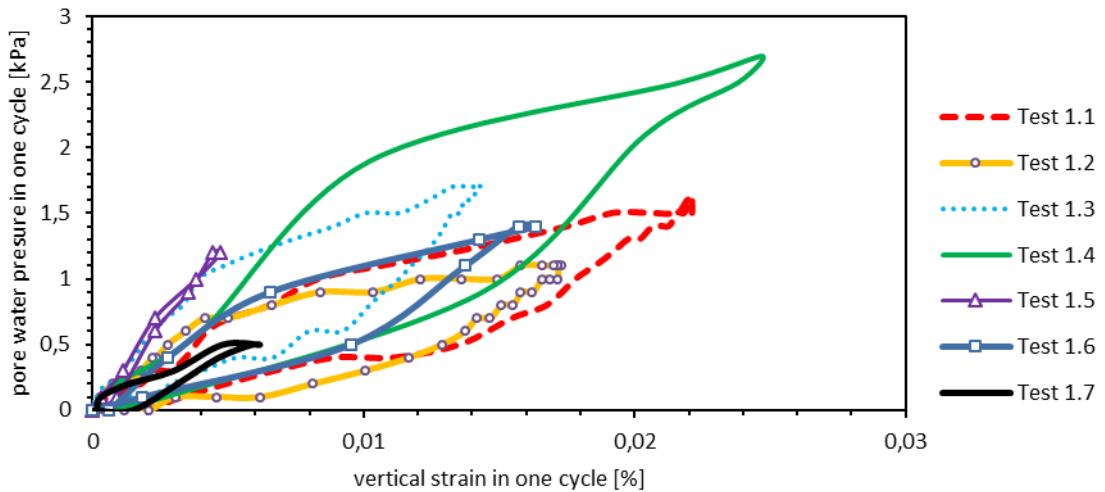
Figure 9. *Excess pore water pressure versus vertical strain for $1 \cdot 10^3$ cycle of loading in cyclic triaxial tests for all seven tests.*

The excess pore water pressure varies from 0.5 kPa to 2.7 kPa. The greatest Δu value was observed in the case of test 1.4 where the failure of the sample was observed. The lowest value of vertical strain was observed in the case of test 1.5. This test characterises itself with low–stress amplitude and with high initial void ration e_0 equal to 0.59. In order to characterise the impact of test conditions stored in Table 1 on the excess pore water pressure in the cycle $1 \cdot 10^3$ the statistical analysis was conducted. Table 3 presents data concerning the Δu and ε_1 in seven tests for cycle $1 \cdot 10^3$.

Table 3. Excess pore water pressure and vertical strain data for cycle $1 \cdot 10^3$.

Test No.	Δu_{avg} [kPa]	Δu_a [kPa]	$\varepsilon_{1, avg}$ [%]	$\varepsilon_{1, a}$ [%]
1	27.70	0.80	0.8325	0.0111
2	29.55	0.55	0.8482	0.0085
3	43.55	0.85	0.5367	0.0072
4	12.45	1.35	0.3559	0.0123
5	19.40	0.30	0.3201	0.0023
6	21.40	0.70	0.6512	0.0082
7	23.75	0.25	0.3128	0.0030

where, Δu_{avg} – excess pore water pressure average in cycle, Δu_{avg} – excess pore water pressure amplitude ($\Delta u_{avg} = \Delta u_{max} - \Delta u_{min}$), $\varepsilon_{1, avg}$ – vertical strain average, $\varepsilon_{1, a}$ – vertical strain amplitude.

For the presented above data, the multiple linear regression test was conducted. The statistical analysis was performed in order to establish the relationship between the factors which might impact on the excess pore pressure value.

For average excess pore water pressure Δu_{avg} the statistical regression was established between deviator stress median q_m, initial minor principal effective stress σ'_3 and initial void ratio e_0. The dependence has the following form:

$$\Delta u_{avg} = -20.059 + 0.688q_m + 0.17\sigma'_3 + 26{,}751e_0$$

(1)

Where, q_m and σ'_3 are in (kPa) and e_0 in (–). The above presented formula has coefficient of determination R^2 equal to 0.931 which indicates a high correlation between data and results of the calculation based on Eq. (1). The standard error of estimation is equal to 3.624 and for P <0.05 the Eq.(1) have ability to predict Δu_{avg} value.

For the Δu_a the multiple linear regression test was performed as well. For this analysis, the additional two factors was applied namely, the amplitude of deviator stress q_a and the Δu_{avg} value. The formula has the following form:

$$\Delta u_a = -1.272 - 0.129q_m - 0.0137\sigma'_3 - 1.596e_0 + 0.872q_a + 0.085\Delta u_{avg}$$

(2)

Where, q_a is in (kPa). This formula has the coefficient of determination R^2 equal to 0.995 which indicates high correlation between data and results of the calculation based on Eq. (2). The standard error of estimation is equal to 0.067.

The excess pore water pressure is therefore dependent from initial soil skeleton condition which is governed in this study by initial void ratio and initial stress state which is represented by, initial minor principal effective stress σ'_3 and

also by deviator stress parameters. The Eq. (1) and (2) can be applied for calculations of excess pore water pressure of tested kind cohesive compacted soils (sasiCl) in such conditions of stress state.

4 CONCLUSIONS

In this article, the compacted cohesive soil (sasiCl) was studied subjected to long-term cyclic loading. The excess pore water pressure was analysed in terms of vertical strain. The analysis of the test results has led to the following conditions:

1. Excess pore water pressure develops during cyclic loading in a different manner which is dependent on stress state and physical factors.
2. The highest pore pressure in cycle was observed for soil samples with the lowest initial void ratio what indicates that well–compacted soils are more likely to develop high excess pore water pressure during cyclic loading.
3. The average excess pore water pressure Δu_{avg} and Δu_a depends from initial void ratio and initial stress state which is represented by, initial minor principal effective stress σ'_3 and also by deviator stress parameters.
4. The pore pressure development during cyclic loading is an important parameter to know for designers. The cohesive soil failure or high deformation during traffic is highly undesirable. Therefore, the Eq. (1) and (2) can be used in the analysis of cyclic loading impact on the excess pore water pressure generation for sandy silty clays.

5 ACKNOWLEDGEMENTS

6 REFERENCES

Ansal, A. M., Erken, A. 1989. Undrained behavior of clay under cyclic shear stresses. *J. Geotech. Engrg.* **115(7)**, 968–983.

Bayraktaroglu, H., Taşan, H. E. 2018. Effects of sandy soils permeability variation on the pore pressure accumulation due to cyclic and dynamic loading. *In: Numerical Methods in Geotechnical Engineering IX, Volume 1: Proceedings of the 9th European Conference on Numerical Methods in Geotechnical Engineering (NUMGE 2018)*, Porto, Portugal (p. 443). CRC Press.

Booker, J.R., Rahman, M.S. Seed, H.B. 1976. GADFLEA – A Computer Program for the Analysis of Pore Pressure Generation and Dissipation During Cyclic or Earthquake Loading. EERC 76-24. University of California, Berkeley.

Brown, S. F., Lashine, K. F., Hyde, A. F. L. 1975. Repeated load triaxial testing of a silty clay. *Geotechnique* **15(1)**, 95–114.

Cary, C. E., Zapata, C. E. 2016. Pore water pressure response of soil subjected to dynamic loading under saturated and unsaturated conditions. *International Journal of Geomechanics*, **16(6)**, D4016004.

Fredlund, D. 2006. Unsaturated soil mechanics in engineering practice. *J. Geotech. Geoenviron. Eng.*, **132(3)**, 286–321.

Głuchowski, A., Szymański, A., Sas, W. 2015. Repeated loading of cohesive soil–

shakedown theory in undrained conditions. *Studia Geotechnica et Mechanica* **37(2)**, 11-16.

Green R.A., Mitchell, J.K., Polito, C.P. 2000. An Energy-Based Excess Pore Pressure Generation Model for Cohesionless Soils In: *Proceedings of the John Booker Memorial Symposium Sydney, New South Wales*, Australia, A.A. Balkema Publishers, Rotterdam, Netherlands (2000), 1-9

Hsu, C., Vucetic, M. 2006. Threshold shear strain for cyclic pore-water pressure in cohesive soils. J. *Geotech. Geoenviron. Eng.* **132(10)**, 1325–1335.

Ichii, K. Mikami, T. 2018. Cyclic threshold shear strain in pore water pressure generation in clay in situ samples. *Soil and Foundations* **58(3)**, 756-765.

Leng, J., Liao, C., Ye, G., Jeng, D. S. 2018. Laboratory study for soil structure effect on marine clay response subjected to cyclic loads. *Ocean Engineering* **147**, 45-50.

Mendoza, M. J., Hernandez, V. M. 1994. Pore-pressure build-upunder cyclic loading in Mexico City clay. *Proc., 13th Int. Conf. on Soil Mechanics and Foundations Engineering*, CRC Press, Boca Raton, FL,181–186.

PN-EN 14688:2006/Ap1 : Badania geotechniczne Oznaczanie i klasyfikowanie gruntów Część 1: Oznaczanie i opis

Sun, L. 2018. Effect of Cyclic Stress Level and Overconsolidation Ratio on Permanent Deformation Behaviour of Clayey Subsoil. *Civil Engineering Journal*, **4(8)**, 1772-1782.